

12 Abstract

13 We developed a one-dimensional model to estimate salp contributions to vertical carbon flux at the
14 Bermuda Atlantic Time-series Study (BATS) site in the North Atlantic subtropical gyre for a 17-yr period
15 (April 1994 to December 2011). We based the model parameters on published rates of salp physiology
16 and experimentally determined sinking and decomposition rates of salp carcasses. Salp grazing was low
17 during non-bloom conditions, but routinely exceeded 100% of chlorophyll standing stock and primary
18 production during blooms. Fecal pellet production was the largest source of salp carbon flux (78% of
19 total), followed by respiration below 200m (19%), sinking of carcasses (3%), and DOC excretion below
20 200m (<0.1%). *Thalia democratica*, *Salpa fusiformis*, *Salpa aspera*, *Wheelia cylindrica*, and *Iasis*
21 *zonaria* were the five highest contributors, accounting for 95% of total salp-mediated carbon flux.
22 Seasonally, salp flux was higher during spring-summer than fall-winter, due to seasonal changes in
23 species composition and abundance. Salp carbon export to 200m was on average 2.3 mg C m⁻² d⁻¹ across
24 the entire time series. This is equivalent to 11% of the mean 200m POC flux measured by sediment traps
25 in the region. Salp blooms were particularly productive, accounting for 79% of the total modeled salp
26 POC flux at 200m across the time series. Salp carbon flux attenuated slowly, and at 3200m the average
27 modeled carbon from salps was 109% of the POC flux measured in sediment traps at that depth.
28 Migratory and carcass carbon export pathways should also be considered (alongside fecal pellet flux) as
29 facilitating carbon export to sequestration depths in future studies.

30 Keywords: Salps, Thaliacea, Carbon export, Sargasso Sea, Biological Pump, fecal pellet

31

32

33

34

35

36

37 Introduction

38 The Sargasso Sea is an oligotrophic region in the North Atlantic subtropical gyre, with patterns in
39 biogeochemistry influenced by physical forcing, moderated by strength of winter mixing, and tied to
40 decadal-scale climate oscillations (Saba et al. 2010, Álvarez-García et al. 2011, Wu et al. 2011). In years
41 with increased frequency of winter mixing, increased surface nutrients fuel new production, ultimately
42 leading to higher particulate organic carbon fluxes to 150 m (Lomas et al. 2010). As this mass flux
43 continues to sink, organic carbon content decreases from 11.4% of the total at 500m to only 4.6% at
44 3200m, indicating high remineralization by bacteria and deep-sea zooplankton (Conte et al. 2001),
45 although physical fragmentation of larger particles into smaller, non-sinking particles may also occur. In
46 the Sargasso Sea, flux to the meso- and bathypelagic zones consists of phytodetritus, amorphous
47 aggregates, zooplankton fecal pellets, and foraminifera shells (Shatova et al. 2012, Conte & Weber 2014),
48 with variation in mass flux closely coupled to seasonal changes in epipelagic particle flux (Conte et al.
49 2001, Lomas et al. 2010). Flux is also influenced by climate oscillations, with higher nitrogen flux to
50 3200m in years with a negative North Atlantic Oscillation (NAO) anomaly (Conte & Weber 2014).
51 Interannual variations in mesozooplankton biomass in this region also affect vertical export (Steinberg et
52 al. 2012); we examine here how fluctuations in salp populations (Stone and Steinberg 2014) contribute to
53 vertical carbon flux through a variety of mechanisms.

54 Salps are gelatinous, tubular zooplankton which alternate life stages between solitary, sexually-
55 produced individuals and aggregated, asexually-produced colonies—ranging in size from a few mm's to
56 tens of m's in length. Salps are highly efficient filter feeders, with clearance rates up to several liters salp⁻¹
57 hour⁻¹ (Madin and Cetta 1984, Andersen 1985, Vargas and Madin 2004), and they can consume a broad
58 size range of phytoplankton and bacteria (Bone et al. 2003, Sutherland et al. 2010). Salps feed incessantly
59 as they propel themselves through the water, and when numerous, can consume up to 3.5% of the
60 chlorophyll standing stock (Hereu et al. 2006). Their continuous ingestion of a wide range of particle
61 sizes promotes rapid rates of growth, reproduction, and defecation. Salp fecal pellets are relatively large

62 (Caron et al. 1989, Sutherland et al. 2010), and sink at rates up to 1600m day⁻¹ (Bruland and Silver 1981,
63 Phillips et al. 2009). Due to fast sinking velocities, salp pellets can reach bathypelagic depths relatively
64 intact, and are found in high numbers in sediment traps (Iseki 1981, Matsueda et al. 1986, Caron et al.
65 1989, Conte et al. 2001). This observation suggests remineralization or scavenging of these particles by
66 microbes or other metazoans may be limited.

67 Dead carcasses of salps also contribute to vertical export of organic matter (Lebrato et al. 2013a).
68 While the fate of many salp blooms is unknown, seasonal blooms of salps often quickly collapse (Purcell
69 et al. 2001), and this sudden production of carcasses can represent an important source of food for deep-
70 sea animals and bacteria (Cacchione et al. 1978, Wiebe et al. 1979, Lebrato et al. 2012). Flux from salp
71 fecal pellets and carcasses are estimated to contribute up to 72% of the measured flux in the coastal
72 Mediterranean (Andersen and Nival 1988), and a *Salpa* sp. bloom in the northeastern Pacific resulted in a
73 major deposition of fecal pellets and carcasses to the seafloor (Smith et al. 2014). In addition to
74 producing fecal pellets and carcasses, several abundant species of salps in the Sargasso Sea and elsewhere
75 undergo diel vertical migration, spending time well below the pycnocline during the day and migrating to
76 surface waters at night (Wiebe et al. 1979, Madin et al. 1996, Stone and Steinberg 2014). While at depth,
77 vertical migrators metabolize particulate organic carbon (POC) consumed in surface waters, respiring it as
78 CO₂ and excreting dissolved organic carbon (DOC), contributing to vertical transport of carbon to depth
79 (Steinberg et al. 2001).

80 While salps are important contributors to vertical carbon flux while they are present, their
81 populations are quite variable. Salps periodically bloom throughout the world's oceans, including in the
82 Sargasso Sea (Madin et al. 1996, 2001, Roman et al. 2002, Stone and Steinberg 2014), where they are
83 occasionally the dominant epipelagic zooplankton (Stone and Steinberg 2014). Salps are sensitive to
84 interannual and longer-term changes in the environment, mostly related to variations in temperature and
85 stratification. Shifts in prevailing wind led to temperature and primary production changes that caused
86 salp species composition in the Mediterranean to alternate between *Thalia democratica* and *Salpa*

87 *fusiformis* (Ménard et al. 1994, Licandro et al. 2006). Increases in temperature, as measured by the
88 Northern Hemisphere Temperature anomaly, caused observed increases in the pelagic tunicate *Pyrosoma*
89 *atlanticum* due to more stable water masses and decreases in phytoplankton community size (Lebrato et
90 al. 2013b). Long-term regional changes in salp populations have been reported in the California Current
91 (Lavaniegos & Ohman 2007) where shifts in temperature regimes caused changes to both their species
92 composition and biomass. In the Southern Ocean, changes in El Niño–Southern Oscillation (ENSO) and
93 regional warming are correlated with increases in salps (Atkinson et al. 2004, Loeb et al. 2010), and
94 worldwide, gelatinous zooplankton fluctuations are linked to oscillations in climate indices (Condon et al.
95 2013). In the Sargasso Sea, biomass of the salps *Thalia democratica* and *Cyclosalpa polae* increased
96 over the last 20 years, and was positively correlated with water column stratification (Stone and Steinberg
97 2014). *T. democratica* abundance was also higher within cyclonic eddies in the Sargasso Sea, possibly
98 through increased eddy-induced production or through eddy-wind aggregation (Stone and Steinberg
99 2014). These long-term changes in salps in the Sargasso Sea could increase carbon export to the deep
100 sea.

101 In this study, we hypothesize that all three mechanisms of salp-mediated carbon export –1)
102 sinking of fecal pellets, 2) sinking of carcasses, and 3) respiration and excretion at depth– represent
103 significant pathways of export. To test this hypothesis, we used salp abundance and species composition
104 data from the Bermuda Atlantic Time-series Study (BATS) to individually model each species’
105 contributions to vertical carbon flux. This one-dimensional model includes previously-published rates of
106 salp fecal pellet production and sinking, newly measured rates of salp carcass decomposition and sinking,
107 and previously published rates of salp metabolism. By modeling each species and export mechanism
108 separately, we can estimate total salp contributions to vertical flux in an oligotrophic, open-ocean
109 environment and how those fluxes change through the water column as salp abundance and species
110 composition change.

111

112 Methods

113 Sinking and decomposition rate experiments

114 Salps used in sinking and decomposition rate experiments were collected in the western North
115 Atlantic subtropical gyre at stations within ~100km of the Bermuda Atlantic Time-series Study (BATS)
116 sampling site (31°40'N, 64°10'W). Cruises were aboard the R/V *Atlantic Explorer* during the 'Trophic
117 BATS' project from July 19-31, 2012 and on regular monthly BATS cruises from March 4-7, April 28 –
118 May 3, and August 19-23, 2014. Salps were collected using a net with a 0.8 x 1.2m rectangular mouth,
119 202 µm mesh, and a non-filtering cod end to minimize damage to the salps. Tows were conducted during
120 both day and night to depths of 50-150m, and lasted ~50 minutes each. Immediately after each tow,
121 captured salps were separated from other zooplankton and brought into the lab for experimentation. Any
122 particles or other zooplankton stuck to the outside or inside of the salps were first removed. Salps were
123 then identified to species and life stage, and individual salp length was measured as the oral-atrial
124 distance using digital calipers. Salps that were not already dead post capture were killed by placing them
125 in a shallow pan of seawater (~2mm deep) to collapse and suffocate them while allowing them to remain
126 moist.

127 To determine sinking rates, dead salps were placed individually into a sinking chamber comprised
128 of a clear acrylic tube 60cm long and 15cm in diameter filled with surface seawater. This experimental
129 set up and sinking chamber is similar to those used in Lebrato et al. (2013a), which were 12.5cm and
130 19cm in diameter. The chamber diameter in relation to the size of some of the salps may allow flow
131 interactions between the salp and the wall, slowing the salp sinking rate. To correct for this, we used
132 equation 12 from Ristow et al. (1997) to apply a sidewall correction factor to each individual salp's
133 sinking rate based on the size of the salp. Water temperature was measured using a Cole-Parmer
134 Traceable® 90205-22 temperature probe, and salinity was determined from the ship's flow-through
135 salinometer. Water temperature in the sinking chamber changed less than 1°C throughout each

136 experimental run, and salps were stored in water with the same temperature and salinity as the sinking
137 chamber. After placement in the sinking chamber using forceps, salps were gently shaken to remove any
138 bubbles on or inside the salps. If any bubbles remained, the salp was discarded. Each salp was then
139 gently released and allowed to sink. Depth of each salp in the sinking chamber was determined by
140 comparison to measurement markings on the outside of the chamber. Once each salp appeared to reach
141 terminal velocity (after ~20cm), a timer was started, and the time to sink a distance between 5 and 30cm
142 was recorded. Different sinking distances were used when an individual salp sank particularly quickly or
143 slowly, as we attempted to time each sinking salp for 30-60 seconds. Each salp was sunk once to avoid
144 retrieving the salp from the bottom of the chamber and introducing turbulence.

145 Decomposition rate experiments were conducted with *Cyclosalpa polae*, *Iasis zonaria*, *S.*
146 *fusiformis*, *S. maxima*, *Thalia democratica*, *Wheelia cylindrica*, and *Ritteriella retracta* in March, May,
147 and August of 2014. Dead salps were placed in small (~5x5cm) 200 μ m mesh bags submerged in a large
148 beaker in the dark with a continuous flow-through of surface seawater (19-23 °C) for the duration of the
149 experiment, simulating the decomposition process in warm epipelagic waters with the resident microbial
150 assemblage. Several salps were removed at each time point from their mesh bags and “sacrificed” from
151 the experiment to be frozen for analysis onshore. This removal occurred at regular intervals (~8-12
152 hours) until all salps were either removed or completely decomposed. Once onshore, salp remains were
153 placed in a drying oven at 60°C for at least one week and then weighed. Initial salp dry weight (i.e., T_0)
154 was estimated from length measurements of freshly caught, whole salps using published salp live length
155 to carbon weight regression equations for each species (see Table 5.3 in Madin & Deibel 1998, and
156 references therein). Occasionally, the measured dry weights of the initial, undecomposed salps were
157 consistently different from the dry weights calculated by the regression equations. When this occurred, a
158 correction factor was applied to all salps in that experiment by adding or subtracting the difference
159 between the mean calculated and mean measured dry weights of the time zero (t_0) salps. Decay rate of

160 salp carcasses was calculated by plotting the percent remaining of initial salp dry weight over time and
161 fitting a first-order exponential decay curve:

$$162 \quad P = a * e^{(-k*t)}$$

163 Where ‘P’ is percent of starting salp dry weight remaining, ‘a’ is the percent remaining at time zero t_0 , ‘k’
164 is the decay constant, and ‘t’ (hours) is time from the start of the experiment. Similar experiments were
165 carried out at 8°C using water collected from 1000m, to simulate meso- and bathypelagic conditions. For
166 these experiments, instead of water continuously flowing through the decomposition chamber, carcasses
167 were placed in 4L bottles in a refrigerator, and the water in each bottle was replenished every 12 hours.

168 Model development

169 We developed a one-dimensional model to calculate salp contributions to total vertical carbon
170 flux (Figure 1). Fecal pellet production, grazing, production of carcasses, and respiration at depth was
171 calculated daily for each species’ biomass. Data forced into the model included biological,
172 environmental, and process rate data (e.g., salp biomass, temperature, primary production) collected
173 through the BATS program (<http://bats.bios.edu/>), previously published rates of salp metabolic and export
174 processes (fecal pellet production, respiration, and DOC excretion), as well as results from the above
175 sinking and decomposition experiments. Salp ‘blooms’ were defined as in Stone and Steinberg (2014),
176 i.e., when total salp biomass is in the top 10% of all observations.

177 Salp biomass (mgC m^{-2}) and vertical migration was calculated from monthly and bimonthly tows
178 at the BATS site as detailed in Stone and Steinberg (2014). Species-specific biomass was averaged from
179 duplicate day and night tows, with only the night tow biomass used for species that exhibited diel-vertical
180 migration. Salp blooms are generally short-lived, and typically do not remain at high abundance for
181 several months. Because the duration of each salp bloom could not be accurately estimated from monthly
182 sampling, the biomass data were linearly interpolated between each sampling date to give a biomass
183 estimate for each day from April 15, 1994 to November 14, 2011. This was done for each of the 21

184 species and 4 higher taxa categories (*Pegea* sp., Salpidae, *Salpa* sp., and *Thalia* sp.) in the dataset; the 25
185 biomass time series were then used to force the flux model. Based on Stone and Steinberg (2014), all
186 species were split into those which exhibited diel vertical migration (DVM; *Salpa fusiformis*, *Wheelia*
187 *cylindrica*, *Iasis zonaria*, *S. aspera*, and *Ritteriella retracta*) and those that did not exhibit DVM
188 (*Brooksia rostrata*, *Cyclosalpa affinis*, *C. floridana*, *C. pinnata*, *C. polae*, *Helicosalpa virgula*, *Ihlea*
189 *punctata*, *Pegea bicaudata*, *P. confoederata*, *P. socia*, *Pegea* sp., *S. maxima*, *Salpa* sp., Salpidae, *Thalia*
190 *cicar*, *T. democratica*, *T. orientalis*, *Thetys vagina*, and *Traustedtia multitentaculata*). For each DVM
191 species, an overall average migrating proportion of the biomass was calculated by dividing each sampling
192 date's day biomass by night biomass and subtracting from 1 to obtain a percentage of biomass that was
193 migrating. These percentages were then averaged for each species across the entire time series. For non-
194 DVM species, we calculated the amount of carbon reaching 200m from both fecal pellet production (FPP)
195 and from sinking of carcasses (i.e., the 'passive flux'). For DVM species, we additionally calculated
196 respiration and dissolved organic carbon (DOC) excretion while at depth (i.e., the 'active flux').

197 Fecal pellet production, sinking of dead carcasses, respiration and DOC excretion at depth, and
198 grazing were all resolved daily from April 1994 to November 2011 as described in the following sections.
199 For fecal pellet production, species-specific FPP rates were used when available from the literature; for
200 species without a specific rate, rates from the same genus or family were averaged (Supplementary Table
201 1; Deibel 1982, Madin 1982, Mullin 1983, Small et al. 1983, Cetta et al. 1986, Andersen 1985, Huntley et
202 al. 1989, Madin and Purcell 1992, Sreekumaran Nair et al. 1995). Fecal pellet decomposition was based
203 on rates averaged from Caron et al. (1989), who measured the loss of ash free dry weight over a 10-day
204 experiment. Based on literature values for fecal pellet sinking rates (Bruland and Silver 1981, Caron et al.
205 1989, Phillips et al. 2009), salp fecal pellets would reach the Sargasso Sea floor well within 10 days.
206 Because the experiments in Caron et al. (1989) looked at fecal pellet decomposition over a total of 10
207 days through a temperature gradient (1 day at 22°C followed by 9 days at 5°C) and did not measure pellet
208 decomposition at only one temperature, we were unable to separately model the decomposition taking

209 place in the warm surface waters from that at colder depths. Thus, we applied the total 10-day
210 decomposition measured by Caron et al. (1989), and no additional decomposition parameter was applied
211 after the fecal pellets reached 200m. Because fecal pellets would sink below 200m much more quickly
212 than 10 days, our estimates are conservative. For DVM species, we assumed the following: 1) FPP was
213 the same in the surface waters and at depth, as salps with full guts would continue to produce fecal pellets
214 after migrating to depth for some time and would not immediately begin producing them again after
215 returning to the surface, 2) migrators spent 12 hours per day above 200m and 12 hours per day below
216 200m, and 3) while physical breakup or resuspension of fecal material may occur, we had no reliable
217 estimates of these processes, and they were not included in the model.

218 We modeled carcass sinking and decomposition by incorporating the experimentally-determined
219 rates for each species (Figure 2 and Table 1), and averaging across genus or family when species-specific
220 rates were not available. Daily biomass of each species and life stage was multiplied by the proportion
221 dying each day (the mortality rate), which gave a biomass of dead salps produced each day. All salps
222 were conservatively assumed to have died at the surface, and the amount of time required to sink 200m
223 was calculated by using the species-specific corrected rates in Figure 2. The decomposition equations in
224 Table 1 were then used with the time required to sink 200m to determine the sinking carcass biomass.
225 The monthly proportion of salp biomass in each life stage (blastozoid or oozoid) was calculated from
226 BATS count data, and then linearly interpolated to obtain a daily value. Life spans were estimated as 3
227 days for *Thalia* blastozoids, 14 days for *Thalia* oozoids, 15 days for all other salp blastozoids, and 30
228 days for all other salp oozoids (Henschke et al. 2011, Deibel and Lowen 2012). Daily death rates were
229 estimated as the proportion of the population reaching the end of its lifespan each day; for example, the
230 14-day lifespan of *Thalia* oozoids translates as 1/14 of *Thalia* oozoid biomass dying each day. For DVM
231 species, we estimated that half of the population died above 200m, and half below 200m. Since we did
232 not measure decomposition at colder temperatures or under increased pressure at depth, we calculated
233 biomass of carcasses produced below 200m (reaching depths of 300m, 500m, 1500m, and 3200m) by

234 applying the decomposition rates of Lebrato et al. (2011, 2013a) separately to *T. democratica* (due to
235 slower sinking speeds of this species), and then to all other species combined. We assumed a constant
236 temperature of 18°C from 200-500m, 8°C from 500-1000m, 5°C from 1000-1500m, and 3°C from 1500-
237 3200m (<http://batsftp.bios.edu/BATS/ctd/>).

238 Salp active transport–respiration and DOC excretion at depth– was calculated for the five DVM
239 species while they were below 200m. One rate for each parameter was applied to all species. An average
240 respiration rate (2.2% body C h⁻¹) was calculated from data compiled in Madin and Purcell (1992) and
241 Cetta et al. (1986). There is no published DOC excretion rate of salps, thus DOC excretion rate for this
242 model was averaged from those of other gelatinous zooplankton (ctenophores and cnidarians) in Condon
243 et al. (2011) (0.182 mgC h⁻¹ g dry body weight⁻¹).

244 Daily salp grazing (mgC m⁻³ d⁻¹) was calculated by multiplying the volume of water cleared by
245 the average carbon biomass of phytoplankton 0-140m, as phytoplankton biomass is not significant below
246 140m. Both daily chlorophyll *a* and primary production were linearly interpolated from the monthly
247 BATS sampling (http://batsftp.bios.edu/BATS/bottle/bats_pigments.txt and
248 http://batsftp.bios.edu/BATS/production/bats_production.dat). Phytoplankton carbon biomass was
249 calculated by multiplying the daily chlorophyll *a* concentration by a seasonal carbon to chlorophyll ratio
250 (C:Chl). These C:Chl ratios (g/g) were calculated from seasonal averages of BATS chlorophyll *a*
251 concentration and average seasonal values of phytoplankton carbon from Wallhead et al. (2014), and were
252 as follows (months in parentheses): 52 – winter (JFM), 60 – spring (AMJ), 52 – summer (JAS), and 47 –
253 fall (OND). Species-specific clearance rates were used when available; otherwise, average rates for genus
254 or family were used (Supplementary Table 1; Harbison and Gilmer 1976, Harbison and McAlister 1979,
255 Deibel 1982, Mullin 1983, Madin and Cetta 1984, Andersen 1985, Deibel 1985, Reinke 1987, Madin and
256 Purcell 1992, Sreekumaran Nair et al. 1995, Vargas and Madin 2004, Hereu et al. 2010). Because salps
257 are considered non-discriminant filter feeders (Madin 1974) and only cease feeding when their internal
258 filters become clogged at very high phytoplankton concentrations (i.e., above ~1 ug chl *a* L⁻¹, Andersen

259 1985 and Harbison et al. 1986; concentrations rarely reached at BATS), we assumed clearance rates to be
260 constant regardless of phytoplankton concentration. While some DVM species may migrate at different
261 times of the day (Madin et al. 1996), further research is needed to quantify these differences, and all
262 DVM species were assumed to graze 12 hours each 24-hr period in surface waters. All salp grazing rates
263 were based on phytoplankton standing stocks, and FPP rates for this model were independent of
264 calculated grazing (see above). If grazing rates were to be used in an energetic model or to calculate FPP,
265 consumption of microzooplankton (such as dinoflagellates and ciliates shown in Vargas and Madin 2004)
266 would also need to be taken into consideration.

267 Sediment trap flux

268 Sediment trap POC flux data ($\text{mgC m}^{-2} \text{ day}^{-1}$) for sediment traps at 150m, 200m, and 300m from
269 April 1994 to November 2011 were downloaded from the BATS database (bats.bios.edu). Mean POC
270 flux for traps at 500m (1984-1986, 1989-1982, and 1997-1998), 1500m (1984-1992, and 1997-1998), and
271 3200m (1978-1998) was calculated from Table 1 in Conte et al. 2001.

272

273 Results

274 Sinking and Decomposition rates

275 Mean salp carcass sinking rate was measured for 8 species ranging in average size from 8mm *T.*
276 *democratica* to 30mm *S. maxima*. Sinking rates ranged from 414-871 m d^{-1} and 467-1002 m d^{-1} , before
277 and after correcting for wall-interaction effects, respectively (Fig. 2), with a mean (corrected) sinking rate
278 across all species of 727 m d^{-1} ($n=293$). The corrected rates were used throughout the model calculations.
279 There were weak linear correlations between salp length vs. sinking rate ($p<0.001$; $r^2 = 0.21$) and water
280 density vs. sinking rate ($p>0.05$; $r^2 < 0.01$). We posit that sinking rate was not dependent on water density
281 due to the high water content of salp carcasses, and thus there was an equally proportional change in their
282 body density as in the surrounding seawater after adjusting to the new temperature. However, there were

283 significant differences in sinking rate between individual species, with *Wheelia cylindrica* (1002m d⁻¹)
284 and *Salpa maxima* (927m d⁻¹) sinking faster than the two slowest sinking species, *Cyclosalpa polae*
285 (526m d⁻¹) and *Thalia democratica* (467m d⁻¹) (Kruskal-Wallis ANOVA on ranks; Figure 2). Thus, the
286 average rates of similar taxa were used in model calculations, and sinking was not based on salp size or
287 variance in water density.

288 Species-specific decomposition rates were calculated for species with sufficient replication to
289 obtain a significant exponential decay curve (*I. zonaria*, *S. fusiformis*, and *T. democratica*), while an
290 average of all of the warm-water experiments was used to fit a decay curve for the rest of the species
291 (Table 1; Figure 3). No measurable decomposition occurred over 3 days during the cold-water
292 experiments. As described in the methods, actual measured salp weights at t₀ were used to adjust the
293 calculated starting weights. This method was successful, as measured/modeled weight ratio at t₀ was
294 distributed normally (Shapiro-Wilk p=0.132) and the mean was 1.07 (±0.27 SD). Modeled salp
295 decomposition was rapid within the first several hours, with 50% of the starting dry weight lost after only
296 8 hours. Decomposition of the subsequent 49% took much longer, ~44 additional hours, with some salp
297 biomass still present 56 hours into the experiment.

298 Grazing Model

299 Total daily salp grazing was, on average, 0.05 mg chl *a* m⁻³ d⁻¹ (± 0.003 standard error, SE), or
300 26% of the chlorophyll biomass over the 17+ year model run (6,423 days). However, median daily salp
301 grazing was only 0.004 mg chl *a* m⁻³ d⁻¹, or 2% of the chlorophyll biomass; this difference being driven
302 by periodically high salp abundances. Likewise, while salp grazing impact was typically low (an average
303 of 3.9% of the chlorophyll biomass during non-bloom salp abundances), during salp blooms, calculated
304 grazing was an average of 220% of the phytoplankton standing stock present in epipelagic waters (Figure
305 4A). Grazing was also seasonally variable, with elevated mean grazing in spring and early summer
306 (March-June; 6.5 mg C m⁻² d⁻¹) compared to the rest of the year (July-February; 0.7 mg C m⁻² d⁻¹).

307 Annual grazing across the time series was a median of 17% of the annual primary production (Figure 4B),
308 with annual grazing exceeding 100% of the primary production in 1999, 2002, and 2008. Additionally,
309 the proportion of primary production exported by salps was low (<0.5%) for much (86%) of the time
310 series, but increased to as much as 35% during large blooms (Figure 5B). On average, 0.5% of all
311 primary production at BATS, from April 1994 to November 2011, was exported to below 200m by salps.

312 Flux Model Results

313 The daily salp-mediated carbon flux to 200m for each of 25 salp taxa from April 15, 1994 to
314 November 15, 2011 was computed in the model. This included fecal pellet production (FPP) and export,
315 sinking of salp carcasses, and respiration and DOC excretion by DVM at depth. The total carbon flux
316 was generally low, with salp-mediated carbon export less than $1.0 \text{ mgC m}^{-2} \text{ day}^{-1}$ in 76% of the time
317 series. However, due to the population dynamics of salps, this low baseline was punctuated with large
318 salp blooms causing spikes in the flux of several orders of magnitude (Figure 5). These salp blooms
319 cumulatively accounted for 79% of the total modeled salp POC flux across the time series, over half of
320 which was produced by the blooms in 1999, 2008, and 2011. Total salp-mediated export to 200m was
321 highly correlated with total salp grazing (Pearson's correlation coefficient = 0.93, $p < 0.001$), and
322 averaged across the entire time series salp carbon flux was 1.6% of the total carbon grazed by salps. The
323 average daily salp-mediated carbon export across the time series was $2.3 \text{ mgC m}^{-2} \text{ day}^{-1}$ and the median
324 flux was $0.4 \text{ mgC m}^{-2} \text{ day}^{-1}$. The largest proportion of salp-mediated carbon export came from fecal
325 pellets, with an annual average of 78% ($586 \text{ mgC m}^{-2} \text{ year}^{-1}$) (Table 2). The second largest contribution
326 to export was from respiration at depth (19%; $139 \text{ mgC m}^{-2} \text{ year}^{-1}$), followed by sinking of carcasses (3%;
327 $23 \text{ mgC m}^{-2} \text{ year}^{-1}$), and DOC excretion at depth (< 0.1%; $0.1 \text{ mgC m}^{-2} \text{ year}^{-1}$) (Table 2).

328 Seasonal trends in salp carbon flux varied according to the source of the flux, and trends were
329 slightly different dependent upon whether mean or median values of export were considered (Fig. 6). As
330 salp export is several orders of magnitude higher during periodic salp blooms, mean values were much

331 higher than median values for much of the model output. Mean export due to salp fecal pellets was
332 elevated in spring and early summer (March-June), while respiration and carcass carbon flux were more
333 elevated in late summer (July-September) (Figure 6A). Median fecal pellet and carcass fluxes were
334 elevated through all of the spring and summer (February-September), while median respiration peaked in
335 late winter (February and March) and summer (July-September) (Figure 6B). DOC excretion was
336 negligible in all seasons. Both mean and median total salp carbon flux were higher in spring and summer
337 than in fall and winter.

338 Five species accounted for 96% of the total salp-mediated carbon flux at BATS, with *Thalia*
339 *democratica* contributing the most, followed by *Salpa aspera*, *S. fusiformis*, *Iasis zonaria*, and *Wheelia*
340 *cylindrica* (Figure 7A). The other 20 species and taxa combined contributed the remaining 4%. This was
341 calculated by summing the total flux contributed by each species for the entire time series. However,
342 when each species' annual total contribution was averaged for each year of 1995-2010, *S. fusiformis* was
343 the largest contributor to flux, followed by *T. democratica*, *S. aspera*, *W. cylindrica*, and *I. zonaria*
344 (Figure 7B).

345 Overall, total annual salp carbon flux ranged widely, from 97 to 4580 mgC m⁻² y⁻¹ in 1997 and
346 1999, respectively (Figure 8A), with a mean and standard deviation of 748 ± 1133 mgC m⁻² y⁻¹ for the
347 time series. Annual BATS 200m sediment trap flux ranged from 5260 to 9710 mgC m⁻² y⁻¹ in 2005 and
348 2002, respectively (Figure 8B) with a mean and standard deviation of 7530 ± 1050 mgC m⁻² y⁻¹. Annual
349 salp-mediated export flux was equivalent to a mean of 10% ± 15 (range 1-60%) of the 200m sediment
350 trap POC flux over the time series (Figure 8C).

351 While there was no consistent long-term change in total salp C export over the time series ($r^2 <$
352 0.01), there was a periodicity to export. We performed spectral analysis on monthly totals of salp C
353 export to 200m, and the highest spectral densities were found at 9, 12, and 36 months (approximate p-
354 value < 0.001, Bartlett's Kolmogorov-Smirnov statistic, Fuller 1996), indicating total salp carbon export

355 cycles on seasonal (9 months between the late summer and spring blooms), annual, and interannual time
356 scales, respectively.

357 Relatively little of the total salp-exported carbon was lost as it sank through the water column
358 (Figure 9), due to fast sinking and slow decomposition of fecal pellets and carcasses. Average daily salp
359 carbon flux at 200m across the time series was $2.3 \text{ mgC m}^{-2} \text{ day}^{-1}$ and only attenuated to $1.9 \text{ mgC m}^{-2} \text{ day}^{-1}$
360 at 3200m. This was a decrease of only 19%, whereas average daily POC flux captured in sediment traps
361 decreased by 92% between 200m and 3200m (from 20.6 to $1.7 \text{ mgC m}^{-2} \text{ day}^{-1}$). At 3200m, calculated
362 salp carbon (mostly from fecal pellets) was equivalent to 109% of the POC collected in the sediment traps
363 (Figure 9).

364

365 Discussion

366 Carcass Sinking Rates

367 Salp carcass sinking rates varied between 467 and 1002 m d^{-1} , similar to the few previously
368 published measurements. Moseley (1880) recorded a sinking rate of $\sim 860 \text{ m d}^{-1}$ for an unknown species
369 of salp, and Wiebe et al. (1979) reported *Salpa aspera* carcasses sank $240\text{-}480 \text{ m d}^{-1}$. Lebrato et al.
370 (2013a) found *Salpa thompsoni* carcasses sink $800\text{-}1700 \text{ m d}^{-1}$, and other gelatinous zooplankton,
371 including *Cyanea* sp., *Pelagia noctiluca*, *Mnemiopsis leidy*, and *Pyrosoma atlanticum*, had average
372 sinking rates of $400\text{-}1500 \text{ m d}^{-1}$. While Lebrato et al. (2013a) found a positive relationship between salp
373 biovolume and sinking rate, we found no significant relationship overall between salp length and sinking
374 rate but that there were some significant differences between species. In our study the smallest species of
375 salp (*Thalia democratica*) did have the slowest sinking rate. Differences between species in sinking rate
376 other than body size could be related to different relative sizes of the dense, phytoplankton-filled gut or
377 sinking orientation of each individual salp.

378 Decomposition rates

379 Decomposition rates of salps were fast enough that while much of the carcass carbon would be
380 exported out of the epipelagic, very little would reach bathypelagic depths before complete
381 decomposition. We found the exponential decay constant ‘ k ’ of all salp species combined to be 2.2 d^{-1} at
382 $21 \text{ }^\circ\text{C}$, which is close to the calculated k of 2.9 d^{-1} for all gelatinous zooplankton using Equation 2 in
383 Lebrato et al. (2011). However, the decay constant for *Thalia democratica* ($k = 14.5$) was much higher
384 than that calculated for all gelatinous zooplankton in Lebrato et al. (2011). While this may be due to a
385 higher surface area-to-volume ratio of the small *T. democratica* compared to larger salps, decomposition
386 of *T. democratica* was included in Equation 2 of Lebrato et al. (2011), albeit at a lower experimental
387 temperature of 16.5°C (Sempere et al. 2000). Sempere et al. (2000) observed that salp carcasses consist
388 of a quickly decomposing, labile fraction and a more slowly decomposing fraction, which is consistent
389 with our experimental results showing exponential decay.

390 While slow-sinking salp species or small individuals, which make up the majority of salp biomass at
391 BATS, may decompose before reaching the benthos, less common blooms of larger and faster sinking
392 species would be able to reach the deep sea. Additionally, DVM species could die at their daytime
393 mesopelagic residence depth, and thus be more likely to reach the benthos since much of the
394 decomposition occurs in warmer surface waters. While we used a depth horizon of salp DVM of 200m
395 for the purpose of our model, at least one species of salp in the North Atlantic subtropical gyre (*Salpa*
396 *aspera*) migrates to depths $>800\text{m}$ (Wiebe et al. 1979), where temperatures are $\sim 10^\circ\text{C}$ and decomposition
397 much slower. Thus, our estimates of salp carcass carbon export to the deep sea are likely conservative.

398 Grazing

399 Salp grazing had relatively low impact on phytoplankton standing stock and primary production
400 (PP) for much of the year, but periodically extremely high grazing during salp blooms resulted in demand
401 often exceeding phytoplankton supply, with grazing over 100% phytoplankton standing stock and PP.

402 Similarly, salp grazing in the Humboldt Current averaged 16% but was up to 60% of PP (Gonzalez et al.
403 2000), off NW Spain averaged 7% of chlorophyll standing stock but was as much as 77% (Huskin et al.
404 2003), in the California current system ranged from <1 to >100% of daily PP and phytoplankton biomass
405 (Hereu et al. 2006), and in the Eastern Tropical North Pacific ranged from 0.01 to 3.5% of chlorophyll
406 standing stock each day (Hereu et al. 2010). The high grazing impact seen during salp blooms would
407 only be sustained for a short time before phytoplankton standing stocks were depleted, suggesting
408 bottom-up control and a mechanism for the rapid demise of salp blooms (Henschke et al. 2014).

409 Seasonal patterns of grazing by salps were similar to other mesozooplankton at BATS, with
410 elevated grazing in spring compared to the rest of the year. Total mesozooplankton (>64 μm) grazing in
411 the Sargasso Sea was 88 mg C $\text{m}^{-2} \text{day}^{-1}$ in March/April 1990 (82% of PP) and 13 mg C $\text{m}^{-2} \text{day}^{-1}$ in
412 August 1989 (25% of PP) (Roman et al. 1993). In both seasons, salps contributed a similar proportion to
413 the total mesozooplankton grazing, with average salp grazing in both March/April and August 6% of the
414 total grazing reported in Roman et al. (1993).

415 Salp-mediated carbon flux

416 On average, total salp-mediated C flux is significant compared to the POC flux measured by
417 sediment traps at 200m, consistent with previous studies of fecal pellet contributions to carbon flux in the
418 Sargasso Sea (Steinberg et al. 2012) and the temperate North Pacific (Iseki 1981). Annual average salp
419 fecal pellet flux in our study is equivalent to 7.8% of sinking trap POC flux and active transport by DVM
420 is 1.9% of trap POC flux. During blooms, however, salps account for a higher portion of C flux out of the
421 euphotic zone, and high-abundance years can produce total salp-mediated carbon fluxes up to 60% (as in
422 1999) of trap POC flux at 200m. These high fluxes are mostly a result of *Thalia democratica* blooms,
423 where daily total export fluxes reached up to 144 mg C $\text{m}^{-2} \text{d}^{-1}$, and these bloom fluxes are more
424 comparable to those found in coastal regions. For example, Madin et al. (2006) found FPP by *Salpa*

425 *aspera* in the summer in slope waters off New England was 5-91 mgC m⁻² night⁻¹, and Phillips et al.
426 (2009) found *S. thompsoni* produced up to 20mg C m⁻² day⁻¹ in fecal pellets off the Antarctic Peninsula.

427 Dissolved organic carbon flux was low compared to other sources of salp carbon export, likely
428 because the most abundant species, *Thalia democratica*, did not vertically migrate, and any DOC
429 excretion by non-DVM species would remain in the surface waters. However, uncertainties in our
430 applied weight-specific salp DOC excretion rate could lead to underestimates of DOC export. There are
431 limited measurements of DOC excretion by zooplankton, and none for salps. We used DOC excretion
432 rates based on those measured for gelatinous zooplankton by Condon et al. (2011). Kremer (1977) found
433 that DOC excretion by the ctenophore *Mnemiopsis leidyi* is equal to 61% of respiration, and Steinberg et
434 al. (2000) found that average DOC excretion was 31% of respiration for several migrating crustacean
435 zooplankton taxa and a gelatinous polychaete. Using an intermediate DOC excretion rate of 40% of
436 respiration, our estimates of salp DOC export at BATS would increase to 56 mgC m⁻² y⁻¹, or 7% of the
437 yearly total salp-mediated carbon flux. Experimental measurements of salp DOC excretion rates are
438 needed to resolve this issue.

439 Seasonality in average carbon export by salps can be explained by seasonality in salp blooms,
440 with the peaks driven by periodic large blooms. The general pattern of higher flux in late winter and
441 spring, and lower flux in late summer and fall, is consistent with the general pattern of primary production
442 at BATS (Steinberg et al. 2001, Lomas et al. 2013). Higher respiratory DVM flux in the early spring and
443 late summer is due to seasonal increases in large, vertically migrating species like *S. fusiformis* in the
444 spring and *W. cylindrica* in the late summer (Stone and Steinberg 2014). Because biomass of salps
445 increases by several orders of magnitude during blooms, average salp fluxes are often driven by a few
446 large blooms over the time series. Thus when summing across an entire year, the difference between
447 mean and median may not be great; however, when summing across smaller time periods, such as a single
448 season, the difference may be large.

449 Differences between salp species' effect on carbon export are primarily dependent on the size of
450 the salp, due to increases in FPP and respiration rates with body size, and whether they vertically migrate.
451 Vertically migrating species (*Salpa aspera*, *S. fusiformis*, *Wheelia cylindrica*, *Iasis zonaria*, and
452 *Ritteriella retracta*) produce fecal pellets and carcasses and respire at depths already below the
453 pycnocline, not only decreasing the distance they have to sink, but also spending less time in warmer
454 surface waters where bacterial decomposition is faster. Carcasses from small species, such as *Thalia* sp.,
455 not only sink more slowly, but also decompose more rapidly. Thus, a small species such as *T.*
456 *democratica* would overall export less carbon than an equivalent biomass of a larger, vertically migrating
457 species such as *S. aspera*. However, in the Sargasso Sea this difference is often masked by the
458 considerably higher biomass of *T. democratica* blooms compared to all other species.

459 There were no significant long-term trends in total annual salp C export, which is dependent on
460 the frequency and size of blooms, and peaks in export every three years is consistent with a three-year
461 cycle of *Thalia democratica* peak biomass (Stone and Steinberg 2014). However, there is a recorded
462 long-term increase in total sinking POC flux to 150m as measured by sediment traps during the high
463 production winter-spring transition period at BATS (Lomas et al. 2010; although there was no significant
464 increase when averaged over the entire year). Steinberg et al. (2012) also calculated an increase in both
465 fecal pellet POC export and active C transport by diel migrating zooplankton over time due to a long-term
466 increase in BATS mesozooplankton biomass (including an increase in DVM zooplankton biomass). This
467 contrast between increases in winter-spring period trap flux and no change in calculated salp flux may
468 indicate that other, non-salp-mediated pathways of export are as efficient as salp-mediated ones during
469 this period. Comparisons between measured trap flux and calculated flux are further complicated by
470 sediment traps not reliably capturing exported particles from spatially and temporally variable salp
471 blooms.

472 Salps contribute an increasingly higher proportion of C export with increasing depth compared to
473 sinking POC flux measured with sediment traps. At 200m, salp flux only accounts for 11% of the daily

474 POC flux on average. Comparatively, average daily POC flux at 3200m of $1.7 \text{ mg C m}^{-2} \text{ day}^{-1}$ at BATS
475 (Conte et al. 2001) is less than our calculated salp flux of $1.9 \text{ mg C m}^{-2} \text{ day}^{-1}$ at that same depth. This
476 high amount of salp carbon reaching the deep sea has been directly observed on one occasion in the
477 northeastern Pacific, where a *Salpa* sp. bloom deposited large amounts of fecal pellets and carcasses to
478 the seafloor (~4000m) (Smith et al. 2014). However, Shatova et al. (2012) quantified zooplankton fecal
479 pellets in traps at 500, 1500, and 3200m at BATS in 2007, and found that FP carbon only contributed
480 4.6% of the total carbon flux at 3200m, much lower than our calculated values. Additionally, they found
481 that fecal pellets are subject to high rates of recycling and repackaging in the deep water column. Our
482 higher estimates of deep salp export may be explained by: including carcasses—which baffles on sediment
483 traps are likely to exclude, including DVM—which is not measured by sediment traps, and not including
484 scavenging and consumption of salp fecal pellets and carcasses.

485

486 Summary and Conclusion

487 Salp populations in the oligotrophic Sargasso Sea play an important role in transporting carbon
488 from the epipelagic zone to the deep sea. The primary source of salp-mediated carbon flux is the sinking
489 of fecal pellets, but contributions from respiration at depth by diel vertically migrating species and sinking
490 of salp carcasses are also important. Salp carbon flux is relatively low for much of the year, punctuated
491 by several orders of magnitude higher fluxes during periodic population blooms, especially in spring.
492 Salp grazing follows a similar pattern, with relatively low levels of grazing interspersed with removal of
493 100% of phytoplankton standing stock and PP during blooms. *Thalia democratica* is the highest
494 contributor to salp flux, but due to its small size and absence of vertical migration, most of this species'
495 contribution is from sinking fecal pellets. Larger species that vertically migrate (such as *Salpa fusiformis*,
496 *S. aspera*, *Iasis zonaria*, and *Wheelia cylindrica*) respire carbon consumed in the epipelagic in the
497 mesopelagic zone, and produce carcasses at depth that can reach the benthos (Cacchione et al. 1978,

498 Wiebe et al 1979). While low and high periods of salp flux average out to be a small percentage of total
499 flux captured annually in sediment traps at 200m, salp flux contributes a much higher percentage of the
500 total flux in the bathypelagic zone, mostly due to slow decomposition and fast sinking of fecal pellets and
501 carcasses.

502 Future changes in the diversity and abundance of salp populations could affect the efficiency of
503 the biological pump in the Sargasso Sea. As shown in Stone and Steinberg (2014), *Thalia democratica*
504 and *Cyclosalpa polae* populations have increased, and *T. democratica* biomass was three-fold higher
505 within cyclonic eddies than outside eddies. If these population increases continue, carbon flux would
506 significantly increase, especially to the bathypelagic and benthos-carbon sequestration depths.

507

508 Acknowledgements

509 We are grateful to the many Bermuda Atlantic Time-series Study (BATS) technicians involved in the
510 sampling and maintenance of the zooplankton time series over the last 2 decades. We appreciate the
511 support of the officers and crew of the R/V ‘*Weatherbird II*’ and the R/V ‘*Atlantic Explorer*’ for help with
512 sample collection. Special thanks go to Mark Brush for assistance with model development. The BATS
513 zooplankton time series was initially funded by National Science Foundation (NSF) grant OCE-9202336
514 to L. P. Madin, and continued by the BATS program through the NSF Chemical and Biological
515 Oceanography programs (OCE-9301950, OCE- 9617795, and OCE-0326885), and through OCE-
516 0752366 and OCE-1258622 to D.K.S., which funded this current effort. Data collected onboard the
517 ‘Trophic BATS’ cruise was supported by OCE -1090149 to R. Condon. This paper is Contribution No.
518 xxxx of the Virginia Institute of Marine Science, College of William & Mary.

519

520 Literature Cited

- 521 Álvarez-García FJ, Ortiz-Bevia MJ, Cabos-Narvaez WD (2011) On the structure and teleconnections of
522 North Atlantic decadal variability. *J Clim* 24: 2209–2223
- 523 Andersen V (1985) Filtration and ingestion rates of *Salpa fusiformis* Cuvier (Tunicata: Thaliacea): Effects
524 of size, individual weight and algal concentration. *J Exp Mar Biol Ecol* 87: 13-29
- 525 Andersen V, Nival P (1988) A pelagic ecosystem model simulating production and sedimentation of
526 biogenic particles: role of salps and copepods. *Mar Ecol Prog Ser* 44: 37-50
- 527 Atkinson A, Siegel V, Pakhomov E, Rothery P (2004) Longterm decline in krill stock and increase in
528 salps within the Southern Ocean. *Nature* 432: 100–103
- 529 Bone Q, Carre C, Chang P (2003) Tunicate feeding filters. *J Mar Biol Assoc UK* 83: 907–919
- 530 Bruland KW, Silver MW (1981) Sinking rates of fecal pellets from gelatinous zooplankton (Salps,
531 Pteropods, Doliolids). *Mar Biol* 63: 295-300
- 532 Cacchione DA, Rowe GT, Malahoff A (1978) Submersible investigation of outer Hudson submarine
533 canyon. In: Stanley DJ, Kelling F (eds) *Sedimentation in Submarine Canyons, Fans, and Trenches*.
534 Dowden, Hutchinson & Ross, Inc. Stroudsburg, PA, p42-50
- 535 Caron DA, Madin LP, Cole JJ (1989) Composition and degradation of salp fecal pellets: implications for
536 vertical flux in oceanic environments. *J Mar Res* 47: 829–850
- 537 Cetta CM, Madin LP, Kremer P (1986) Respiration and excretion by oceanic salps. *Mar Biol* 91: 529-537
- 538 Condon RH, Duarte CM, Pitt KA, Robinson KL, Lucas CH, Sutherland KR, Mianzan HW, Bogeberg M,
539 Purcell JE, Decker MB, Uye S, Madin LP, Brodeur RD, Haddock SHD, Melej A, Parry GD, Eriksen E,
540 Quiñones J, Acha M, Harvey M, Arthur JM, Graham WM (2012) Recurrent jellyfish blooms are a
541 consequence of global oscillations. *PNAS* 110(3): 1000-1005
- 542 Condon RH, Steinberg DK, del Giorgio PA, Bouvier TC, Bronk DA, Graham WM, Ducklow HW (2011)
543 Jellyfish blooms result in a major microbial respiratory sink of carbon in marine systems. *PNAS* 108(25):
544 10225-10230
- 545 Conte MH, Ralph N, Ross EH (2001) Seasonal and interannual variability in deep ocean particle fluxes at
546 the Oceanic Flux Program (OFP)/Bermuda Atlantic Time Series (BATS) site in the western Sargasso Sea
547 near Bermuda. *Deep-Sea Res II* 48: 1471–1505
- 548 Conte MH, Weber JC (2014) Particle flux in the Deep Sargasso Sea: The 35-year Oceanic Flux Program
549 time series. *Oceanography* 27(1): 142-147
- 550 Deibel D (1982) Laboratory-measured grazing and ingestion rates of the salp, *Thalia democratica* Forskal
551 and *Dolioletta gegenbauri* Uljanin (Tunicata, Thaliacea). *J Plankton Res* 4: 143-153
- 552 Deibel D (1985) Clearance rates of the salp *Thalia democratica* fed naturally occurring particles. *Mar Biol*
553 86: 47-54

- 554 Deibel D, Lowen B (2012) A review of the life cycles and life-history adaptations of pelagic tunicates to
555 environmental conditions. ICES J of Mar Sci 69(3): 358
- 556 Fuller WA (1996) Introduction to Statistical Time Series. John Wiley & Sons, New York, NY, pp. 698
- 557 Godeaux J, Bone Q, Braconnot JC (1998) Anatomy of Thaliacea. In: Bone Q (ed) The biology of pelagic
558 tunicates. Oxford University Press, New York, NY, p 1–24
- 559 Goldthwait SA, Steinberg DK (2008) Elevated biomass of mesozooplankton and enhanced fecal pellet
560 flux in cyclonic and mode-water eddies in the Sargasso Sea. Deep-Sea Res II 55: 1360–1377
- 561 González HE, Sobarzo M, Figueroa D, Nöthig EM (2000) Composition, biomass and potential grazing
562 impact of the crustacean and pelagic tunicates in the northern Humboldt Current area off Chile:
563 differences between El Niño and non-El Niño years. Mar Ecol Prog Ser 195: 201-220
- 564 Harbison GR, Gilmer RW (1976) The feeding rates of the pelagic tunicate *Pegea confoederata* and two
565 other salps. Limnol and Oceanogr 21: 517-528
- 566 Harbison GR, McAlister (1979) The filter-feeding rates and particle retention efficiencies of three species
567 of *Cyclosalpa* (Tunicata: Thaliacea). Limnol and Oceanogr 24: 875-892
- 568 Harbison GR, McAlister VL, Gilmer RW (1986) The response of the salp, *Pegea confoederata*, to high
569 levels of particulate material: starvation in the midst of plenty. Limnol Oceanogr 31: 371–382
- 570 Henschke N, Bowden DA, Everett JD, Holmes SP, Kloser RJ, Lee RW, Suthers IM (2013) Salp-falls in
571 the Tasman Sea: a major food input to deep-sea benthos. Mar Ecol Prog Ser 491: 165–175
- 572 Henschke N, Everett JD, Baird ME, Taylor MD, Suthers IM (2011) Distribution of life-history stages of
573 the salp *Thalia democratica* in shelf waters during a spring bloom. Mar Ecol Prog Ser 430: 49–62
- 574 Henschke N, Everett JD, Doblin MA, Pitt KA, Richardson AJ, Suthers IM (2014) Demography and
575 interannual variability of salp swarms (*Thalia democratica*). Mar Biol 161: 149-163
- 576 Hereu CM, Lavaniegos BE, Gaxiola-Castro G, Ohman MD (2006) Composition and potential grazing
577 impact of salp assemblages off Baja California during the 1997–1999 El Niño and La Niña. Mar Ecol
578 Prog Ser 318: 123–140
- 579 Hereu CM, Lavaniegos BE, Goericke R (2010) Grazing impact of salp (Tunicata, Thaliacea) assemblages
580 in the eastern tropical North Pacific. J Plankton Res 32(6): 785-804
- 581 Huntley ME, Sykes PF, Marin V (1989) Biometry and trophodynamics of *Salpa thompsoni* Foxton
582 (Tunicata: Thaliacea) near the Antarctic peninsula in Austral summer, 1983-1984. Polar Biol 10:59-70
- 583 Huskin I, Elices Ma.J, Anadón R (2003) Salp distribution and grazing in a saline intrusion off NW Spain.
584 J Mar Syst 42: 1-11
- 585 Iseki K (1981) Particulate organic matter transport to the deep sea by salp fecal pellets. Mar Ecol Prog Ser
586 5: 55-60

- 587 Kremer P (1977) Respiration and excretion by the Ctenophore *Mnemiopsis leidyi*. *Mar Biol* 44:1 43-50
- 588 Lavaniegos BE, Ohman MD (2007) Coherence of long-term variations of zooplankton in two sectors of
589 the California Current System. *Prog Oceanogr* 75: 42–69
- 590 Lebrato M, Mendes PJ, Steinberg DK, Cartes JE and others (2013a) Jelly biomass sinking speed reveals a
591 fast carbon export mechanism. *Limnol Oceanogr* 58: 1113–1122
- 592 Lebrato M, Molinero J-C, Cartes J, Lloris D, Mélin F, Beni-Casadella L (2013b) Sinking jelly-carbon
593 unveils potential environmental variability along a continental margin. *PLoS ONE* 8(12): e82070
- 594 Lebrato M, Pahlow M, Oschlies A, Pitt KA, Jones DOB, Molinero JC, Condon RH (2011) Depth
595 attenuation of organic matter export associated with jelly falls. *Limnol Oceanogr* 56(5): 1917-1928
- 596 Lebrato M, Pitt KA, Sweetman AK, Jones DOB, Cartes JE, Oschlies A, Condon RH, Molinero JC, Adler
597 L, Gaillard C, Lloris D, Billett DSM (2012) Jelly-falls historic and recent observations: a review to drive
598 future research directions. *Hydrobiol* 690: 227-245
- 599 Li K, Yin J, Huang L, Shang J, Lian S, Liu C (2011) Distribution and abundance of thaliaceans in the
600 northwest continental shelf of South China Sea, with response to environmental factors driven by
601 monsoon. *Cont Shelf Res* 31: 979–989
- 602 Licandro P, Ibañez F, Etienne M (2006) Long-term fluctuations (1974–1999) of the salps *Thalia*
603 *democratica* and *Salpa fusiformis* in the Northwestern Mediterranean Sea: relationships with
604 hydroclimatic variability. *Limnol Oceanogr* 51: 1832–1848
- 605 Loeb VJ, Hofmann EE, Klinck JM, Osmund HH (2010) Hydrographic control of the marine ecosystem in
606 the South Shetland-Elephant Island and Bransfield Strait region. *Deep-Sea Res II* 57: 519–542
- 607 Lomas MW, Bates NR, Johnson RJ, Knap AH, Steinberg DK, Carlson CA (2013) Two decades and
608 counting: 24-years of sustained open ocean biogeochemical measurements in the Sargasso Sea. *Deep-Sea*
609 *Res II* 93: 16-32
- 610 Lomas MW, Steinberg DK, Dickey T, Carlson CA, Nelson NB, Condon RH, Bates NR (2010) Increased
611 ocean carbon export in the Sargasso Sea linked to climate variability is countered by its enhanced
612 mesopelagic attenuation. *Biogeosciences* 7: 57–70
- 613 Madin LP (1974) Field observations on the feeding behavior of salps (Tunicata: Thaliacea). *Mar Biol* 25:
614 143-147
- 615 Madin LP (1982) Production, composition and sedimentation of salp pellets in oceanic waters. *Mar Biol*
616 67: 39–45
- 617 Madin LP, Cetta CM (1984) The use of gut fluorescence to estimate grazing by oceanic salps. *J Plankton*
618 *Res* 6(3): 475-492
- 619 Madin LP, Deibel D (1998) Feeding and energetics of Thaliacea. In: Bone Q (ed) *The biology of pelagic*
620 *tunicates*. Oxford University Press, Oxford, p 81–103

- 621 Madin LP, Kremer P, Hacker S (1996) Distribution and vertical migration of salps (Tunicata, Thaliacea)
622 near Bermuda. *J Plankton Res* 18: 747–755
- 623 Madin LP, Kremer P, Wiebe PH, Purcell JE, Horgan EH, Nemazie DA (2006) Periodic swarms of the
624 salp *Salpa aspera* in the Slope Water off the NE United States: Biovolume, vertical migration, grazing,
625 and vertical flux. *Deep-Sea Res I* 53: 804-819
- 626 Madin LP, Horgan EF, Steinberg DK (2001) Zooplankton at the Bermuda Atlantic Time-series Study
627 (BATS) station: diel, seasonal and interannual variation in biomass, 1994–1998. *Deep-Sea Res II* 48:
628 2063–2082
- 629 Madin LP, Purcell JE (1992) Feeding, metabolism, and growth of *Cyclosalpa bakeri* in the subarctic
630 Pacific. *Limnol and Oceanogr* 37: 1236-1251
- 631 Matsueda H, Handa N, Inoue I, Takano H (1986) Ecological significance of salp fecal pellets collected by
632 sediment traps in the eastern North Pacific. *Mar Biol* 91: 421-431
- 633 Ménard F, Dallot S, Thomas G, Braconnot JC (1994) Temporal fluctuations of two Mediterranean salp
634 populations from 1967 to 1990. Analysis of the influence of environmental variables using a Markov
635 chain model. *Mar Ecol Prog Ser* 104: 139–152
- 636 Moseley HN (1880) Deep-sea dredging and life in the deep sea III. *Nature* 21: 591-593
- 637 Mullin MM (1983) In situ measurement of filtering rates of the salp, *Thalia democratica*, on
638 phytoplankton and bacteria. *J Plankton Res* 5: 279-288
- 639 Phillips B, Kremer P, Madin LP (2009) Defecation by *Salpa thompsoni* and its contribution to vertical
640 flux in the Southern Ocean. *Mar Biol* 156: 455–467
- 641 Purcell JE, Graham WM, Dumont H (eds) (2001) Jellyfish blooms: ecosystem and societal importance.
642 *Developments in hydrobiology* 155. Kluwer Academic Publishers, Dordrecht
- 643 Reinke M (1987) On the feeding and locomotory physiology of *Salpa thompsoni* and *Salpa fusiformis*.
644 *Rep Polar Res* 36: 89
- 645 Ristow GH (1997) Wall correction factor for sinking cylinders in fluids. *Phys Rev E* 55(3): 2808-2813
- 646 Roman MR, Adolf HA, Landry MR, Madin LP, Steinberg DK, Zhang X (2002) Estimates of oceanic
647 mesozooplankton production: a comparison using the Bermuda and Hawaii time-series data. *Deep-Sea*
648 *Res II* 49: 175–192
- 649 Roman MR, Dam HG, Gauzens AL, Napp JM (1993) Zooplankton biomass and grazing at the JGOFS
650 Sargasso Sea time series station. *Deep-Sea Res I* 40(5): 883-901
- 651 Saba VS, Friedrichs MAM, Carr M-E, Antoine D and others (2010) Challenges of modeling depth-
652 integrated marine primary productivity over multiple decades: a case study at BATS and HOT. *Global*
653 *Biochem Cycles* 24: GB3020, doi:10.1029/2009GB003655

654 Sempéré R, Yoro SC, Wambeke FV, Charrière B (2000) Microbial decomposition of large organic
655 particles in the northwestern Mediterranean Sea: an experimental approach. *Mar Ecol Prog Ser* 198: 61-
656 72

657 Shatova O, Kowec D, Conte MH, Weber JC (2012) Contribution of zooplankton fecal pellets to deep
658 ocean particle flux in the Sargasso Sea assessed using quantitative image analysis. *J Plankton Res* 34(10):
659 905-921

660 Small LF, Fowler SW, Moore SA, La Rosa J (1983) Dissolved and fecal pellet carbon and nitrogen
661 release by zooplankton in tropical waters. *Deep-Sea Res* 30: 1199-1220

662 Smith Jr. KL, Sherman AD, Huffard CL, McGill PR, Henthorn R, Von Thun S, Ruhl HA, Kahru M,
663 Ohman MD (2014) Large salp bloom export from the upper ocean and benthic community response in the
664 abyssal northeast Pacific: Day to week resolution. *Limnol Oceanogr* 59(3): 745-757

665 Sreekumaran Nair SR, Achuthankutty CT, Bhattathiri PMA, Madhupratap M (1995) Feeding behaviour
666 of salp *Thalia democratica* (Thaliacea). *Indian Journal of Marine Sciences* 24: 102-103

667 Steinberg DK, Carlson CA, Bates NR, Goldthwait SA, Madin LP, Michaels AF (2000) Zooplankton
668 vertical migration and the active transport of dissolved organic and inorganic carbon in the Sargasso Sea.
669 *Deep-Sea Res I* 47: 137-158

670 Steinberg DK, Carlson CA, Bates NR, Johnson RJ, Michaels AF, Knap AH (2001) Overview of the US
671 JGOFS Bermuda Atlantic Time-series Study (BATS): a decade-scale look at ocean biology and
672 biogeochemistry. *Deep-Sea Res II* 48: 1405–1447

673 Steinberg DK, Lomas MW, Cope JS (2012) Long-term increase in mesozooplankton biomass in the
674 Sargasso Sea: linkage to climate and implications for food web dynamics and biogeochemical cycling.
675 *Global Biogeochem Cycles* 26: GB1004, doi:10.1029/2010GB004026

676 Stone JP, Steinberg DK (2014) Long-term time-series study of salp population dynamics in the Sargasso
677 Sea. *Mar Ecol Prog Ser* 510: 111-127

678 Sutherland KR, Madin LP, Stocker R (2010) Filtration of submicrometer particles by pelagic tunicates.
679 *Proc Natl Acad Sci USA* 107: 15129–15134

680 Vargas CA, Madin LP (2004) Zooplankton feeding ecology: clearance and ingestion rates of the salps
681 *Thalia democratica*, *Cyclosalpa affinis* and *Salpa cylindrica* on naturally occurring particles in the Mid-
682 Atlantic Bight. *J Plankton Res* 26(7) 827-833

683 Wallhead PJ, Garçon, Casey JR, Lomas MW (2014) Long-term variability of phytoplankton carbon
684 biomass in the Sargasso Sea. *Global Biogeochem Cycles* 28, doi:10.1002/2013GB004797

685 Wiebe PH, Madin LP, Haury LR, Harbison GR, Philbin LM (1979) Diel vertical migration by *Salpa*
686 *aspera* and its potential for large-scale particulate organic matter transport to the deep-sea. *Mar Biol* 53:
687 249-255

688 Wu S, Liu Z, Zhang R, Delworth TL (2011) On the observed relationship between the Pacific Decadal
689 Oscillation and the Atlantic Multi-decadal Oscillation. *J Oceanogr* 67: 27–35

690 Yoon WD, Kim SK, Han KN (2001) Morphology and sinking velocities of fecal pellets of copepod,
691 molluscan, euphausiid, and salp taxa in the northeastern tropical Atlantic. *Mar Biol* 139: 923–928

692

699 Figure and table captions

700 Table 1: Warm-water decomposition rates for three species of salps and for all measured species
701 combined. The equation solves for the percent (P) of the starting salp dry weight remaining after H hours.
702 Decomposition follows an exponential decay curve, with a faster decay rate followed by slower
703 decomposition.

704 Table 2: Average annual carbon flux from the 9 largest contributors to flux and all other species
705 combined. Shown are fluxes of fecal pellets, sinking of dead carcasses, respiration at depth of diel-
706 vertical migrators, and the total of those three categories. Values are in mg carbon m⁻² year⁻¹, and ±
707 standard deviation. DOC excretion is less than 0.1 mgC m⁻² year⁻¹ for all species combined.

708 Figure 1: A summary of the model. Black boxes indicate forced values from BATS data (phytoplankton
709 biomass, salp biomass, and salp diel vertical migration), red boxes indicate modeled rates (grazing, fecal
710 pellet production (FPP), sinking carcasses, respiration, dissolved organic carbon (DOC) excretion, and
711 decomposition) and outputs (shallow and deep salp carbon), and blue arrows indicate carbon flow.

712 Figure 2: Mean carcass sinking rate for eight species of salps, arranged from largest salp on the left to
713 smallest on the right. Blue circles are the wall-interaction corrected values of the measured sinking rates
714 (black circles). Error bars are standard error, and n for each species is in parentheses after name.

715 Figure 3: Percent of starting salp dry weight remaining after decomposing in surface waters. Data from 7
716 species and 96 individuals were used to fit the exponential decay regression. Experiments were carried
717 out in March, May, and August of 2014 using surface water that ranged from 19-23°C.

718 Figure 4: A) Daily chlorophyll a concentration (blue) and calculated amount of chlorophyll a grazed by
719 total salps each day (black). B) Annual primary production (integrated to 140m) from 1995 to 2010
720 (black bars) and calculated percent of that annual PP c grazed by total salps for each year (gray bars).

721 Figure 5: A) Total salp daily carbon flux to 200m (green) and 3200m (blue) at BATS. Total flux is from
722 all salp species and is combined fecal pellet export, sinking of salp carcasses, and respiration and DOC
723 excretion by DVM at depth. Blue lines without corresponding green indicate 3200m flux that is nearly
724 equal to the 200m flux. B) Percent calculated total salp flux of daily primary production (integrated to
725 140m).

726 Figure 6: Seasonal variation in the salp flux to 200m of carcasses (red), fecal pellets (black), respiration
727 below 200m (blue), and DOC excretion below 200m (green). Average (A) and median (B) daily salp
728 carbon flux for each Julian day are shown from the entire time series.

729 Figure 7: The percent of the total salp carbon flux at 200m for each of the top 5 species at the BATS site
730 for (A) the sum of each species' contribution across the entire time series and (B) the average annual
731 percent contribution for years 1995-2010.

732 Figure 8: (A) Annual totals from 1995-2010 for combined salp carbon flux to 200m, and the proportion
733 different sources (fecal pellets, respiration, sinking of dead carcasses, and dissolved organic carbon
734 excretion) contribute to those totals. These totals are compared to (B) the total annual BATS sediment
735 trap flux at 200m by calculating (C) the percent salp flux of the total BATS trap flux at 200m.

736 Figure 9: Depth attenuation of modeled salp carbon flux (black bars) and measured sediment trap flux
737 (red bars). Modeled data are averaged from January 1994 to December 2011; 200 and 300m sediment
738 trap fluxes are from the BATS dataset and averaged from January 1989 to December 2011; and 500,
739 1500, and 3200m sediment trap fluxes are collected from Conte et al. (2001).

740

Species	Equation	R ²	p
<i>Iasis zonaria</i>	$P=108*e^{(-0.033*H)}$	0.67	<0.001
<i>Salpa fusiformis</i>	$P=101*e^{(-0.164*H)}$	0.87	<0.001
<i>Thalia democratica</i>	$P=95*e^{(-0.605*H)}$	0.84	<0.001
All species combined	$P=104*e^{(-0.090*H)}$	0.64	<0.001

Table 1

Species	Fecal Pellets mgC m ⁻² year ⁻¹	Carcasses mgC m ⁻² year ⁻¹	Respiration mgC m ⁻² year ⁻¹	Total mgC m ⁻² year ⁻¹
<i>Thalia democratica</i>	417 ±1160	0.4 ±1.1	0	418 ±1160
<i>Salpa aspera</i>	60.9 ±117	7.6 ±14.0	58.4 ±112	127 ±243
<i>Salpa fusiformis</i>	47.9 ±42.9	6.5 ±5.8	46.0 ±41.2	100 ±90
<i>Iasis zonaria</i>	18.3 ±24.7	3.9 ±5.5	14.5 ±19.6	37 ±50
<i>Wheelia cylindrica</i>	10.4 ±26.7	1.3 ±2.8	18.9 ±48.6	31 ±78
<i>Salpa maxima</i>	13.0 ±50.1	1.1 ±4.3	0	14 ±54
<i>Pegea confoederata</i>	6.7 ±17.6	0.4 ±1.2	0	7.1 ±19
<i>Pegea socia</i>	4.9 ±16.1	0.9 ±3.1	0	5.9 ±19.2
<i>Ritteriella retracta</i>	1.9 ±3.6	0.2 ±0.6	1.3 ±3.1	3.5 ±8.1
Other	4.8 ±5.1	0.6 ±0.5	0	5.3 ±5.5
Total	586 ±1140	23.0 ±19.5	139 ±126	749 ±1130

Table 2

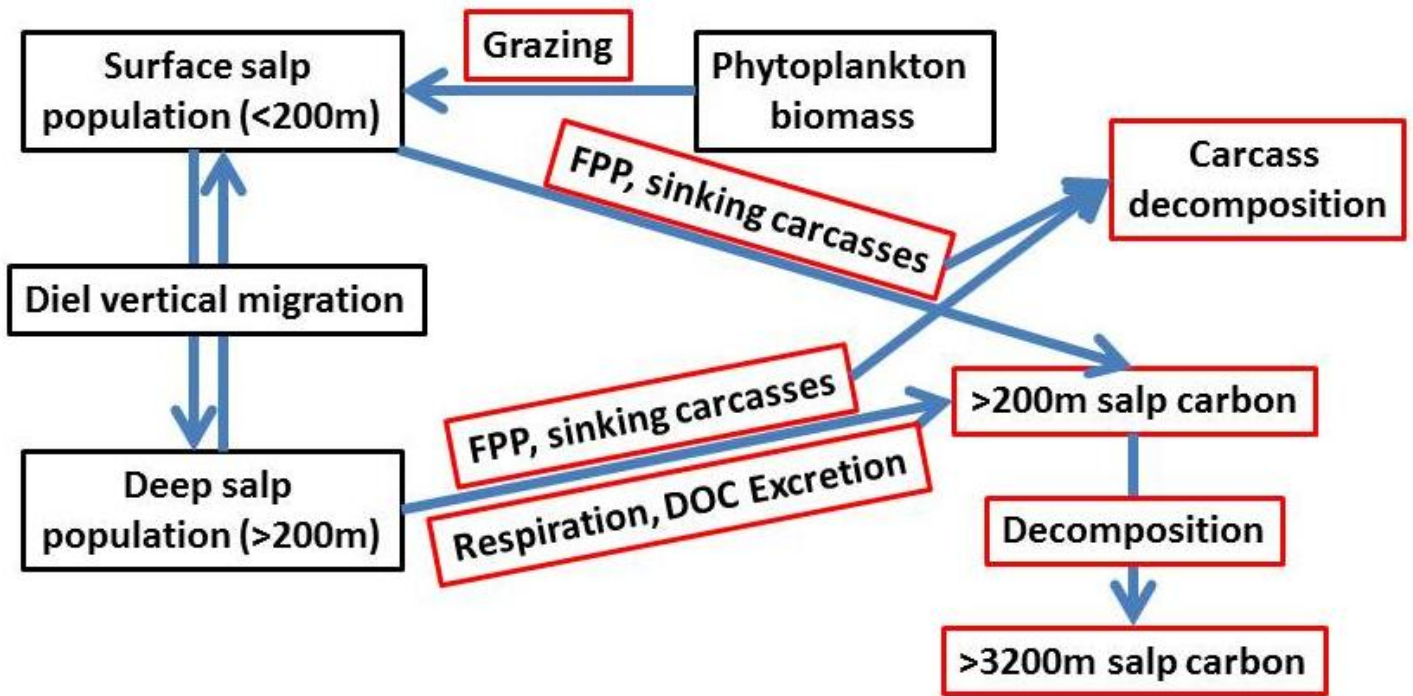


Figure 1

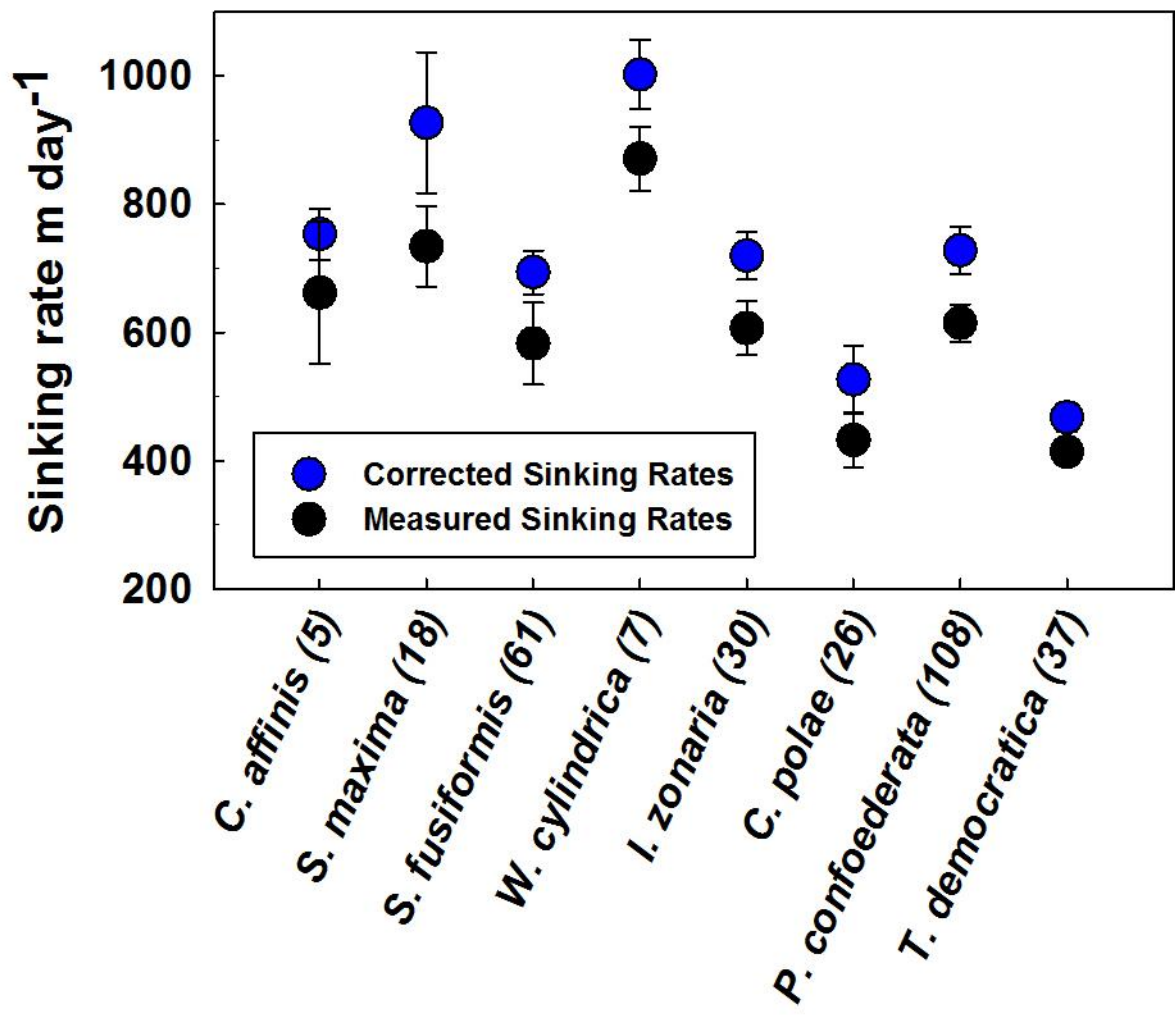


Figure 2

All salps warm water

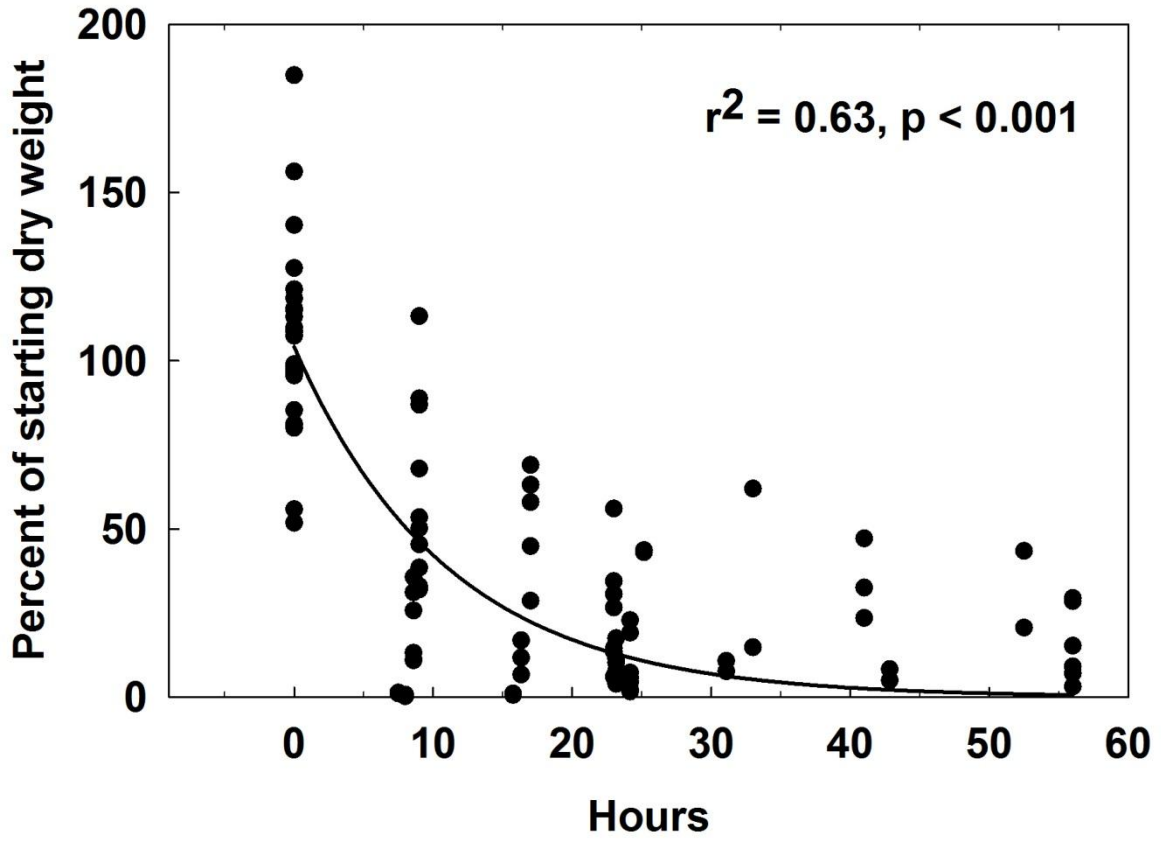


Figure 3

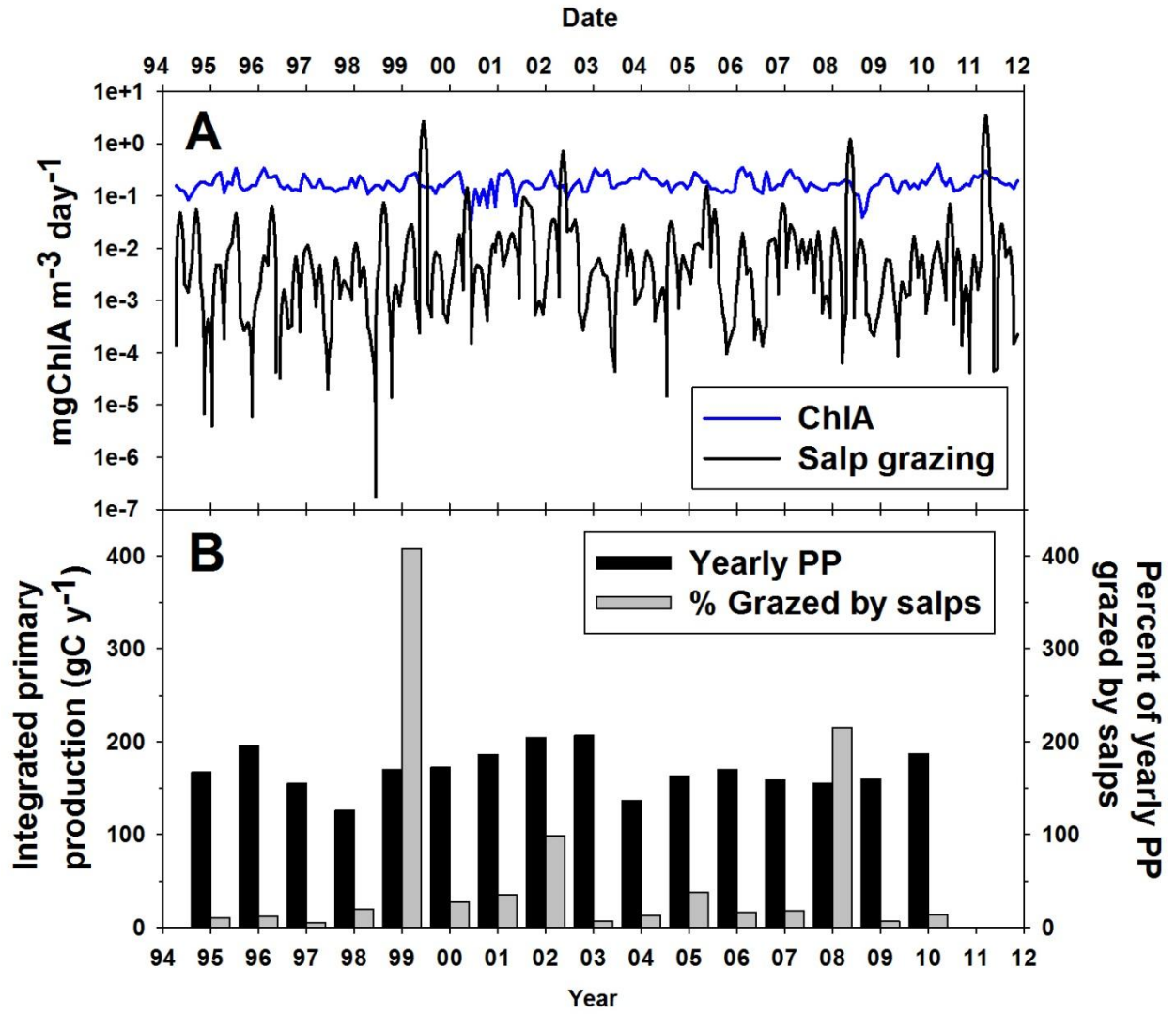


Figure 4

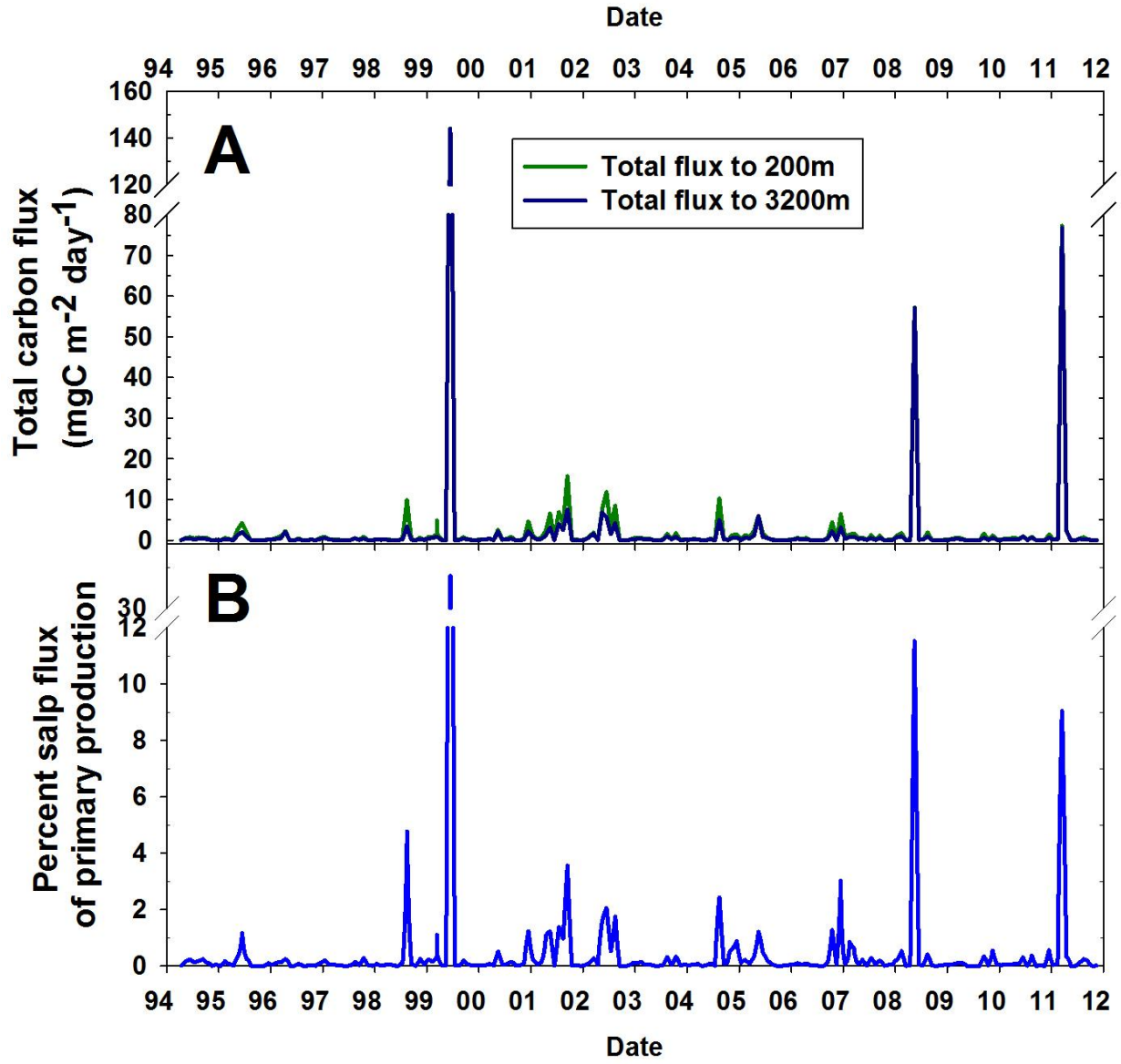


Figure 5

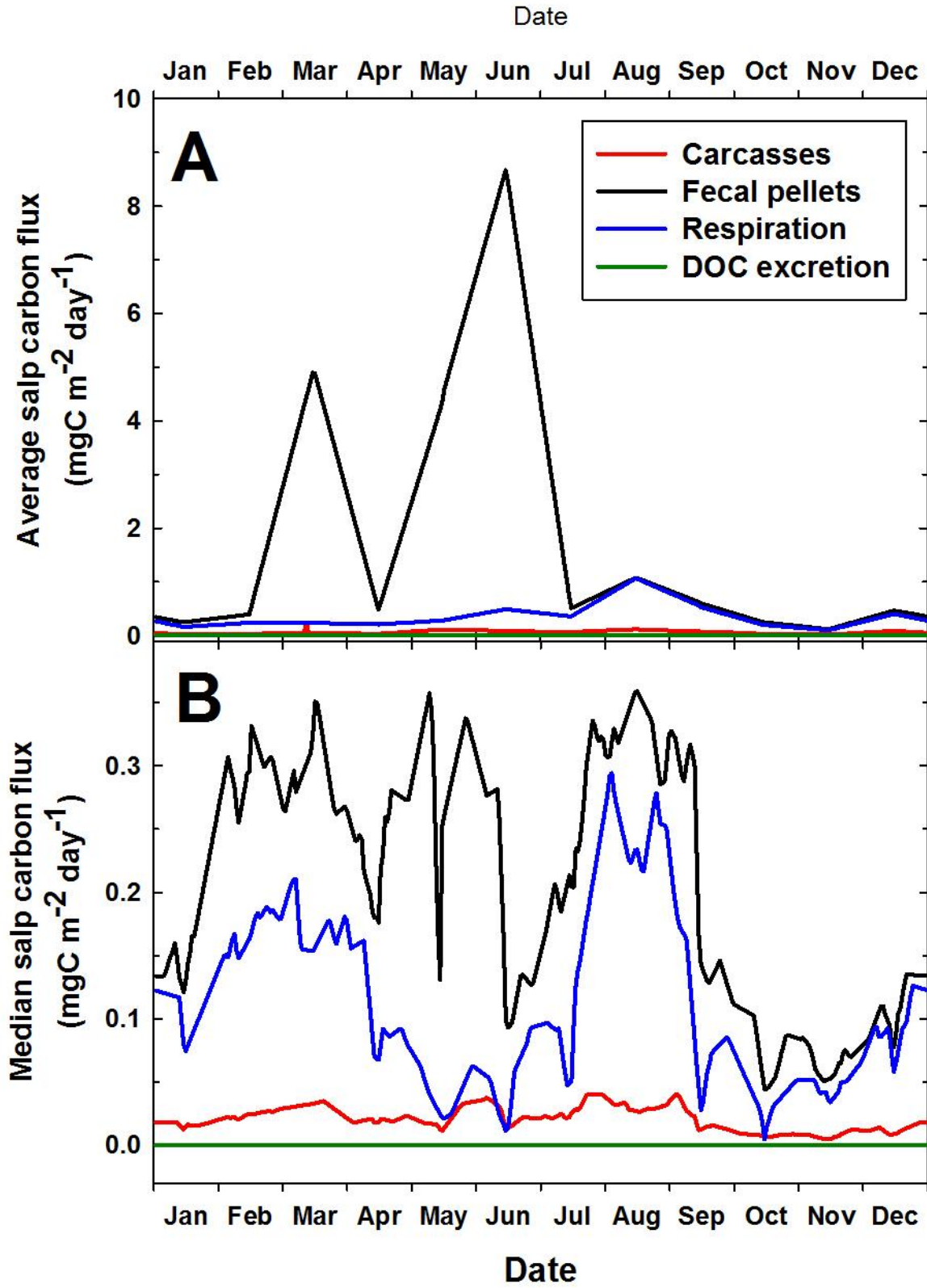


Figure 6

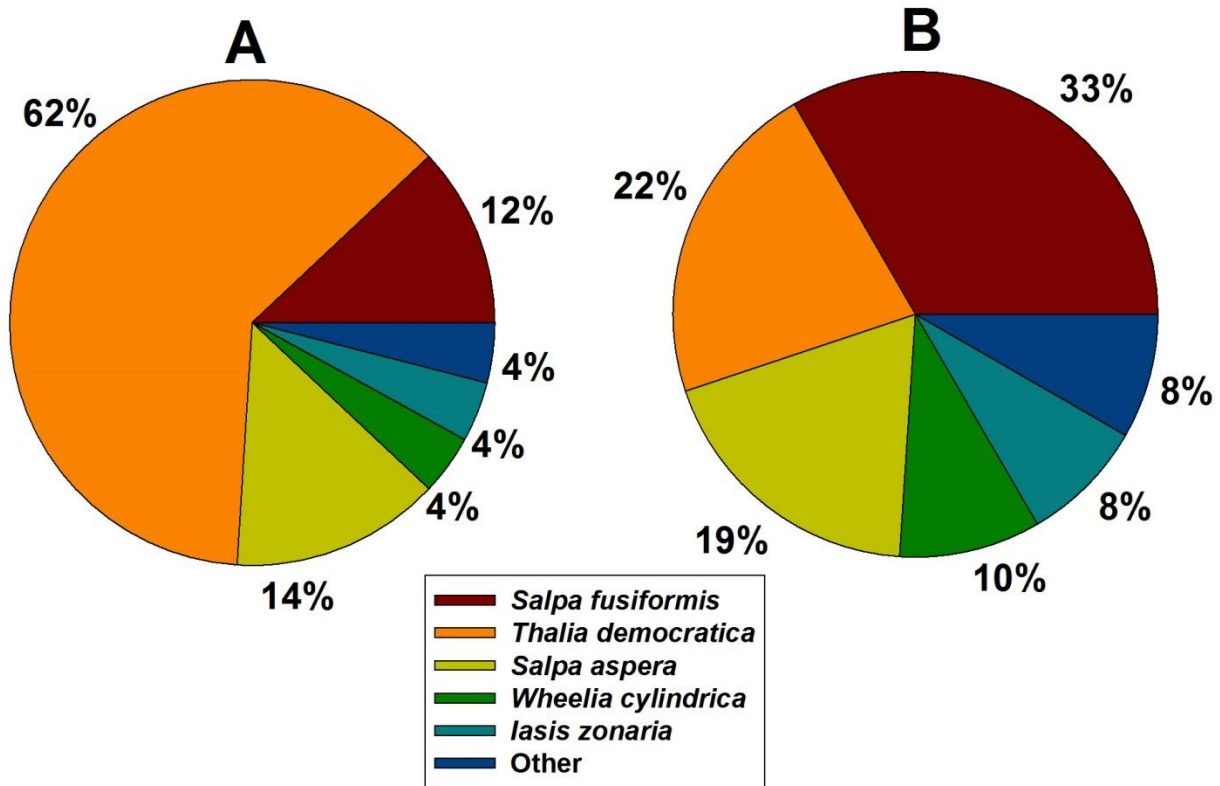


Figure 7

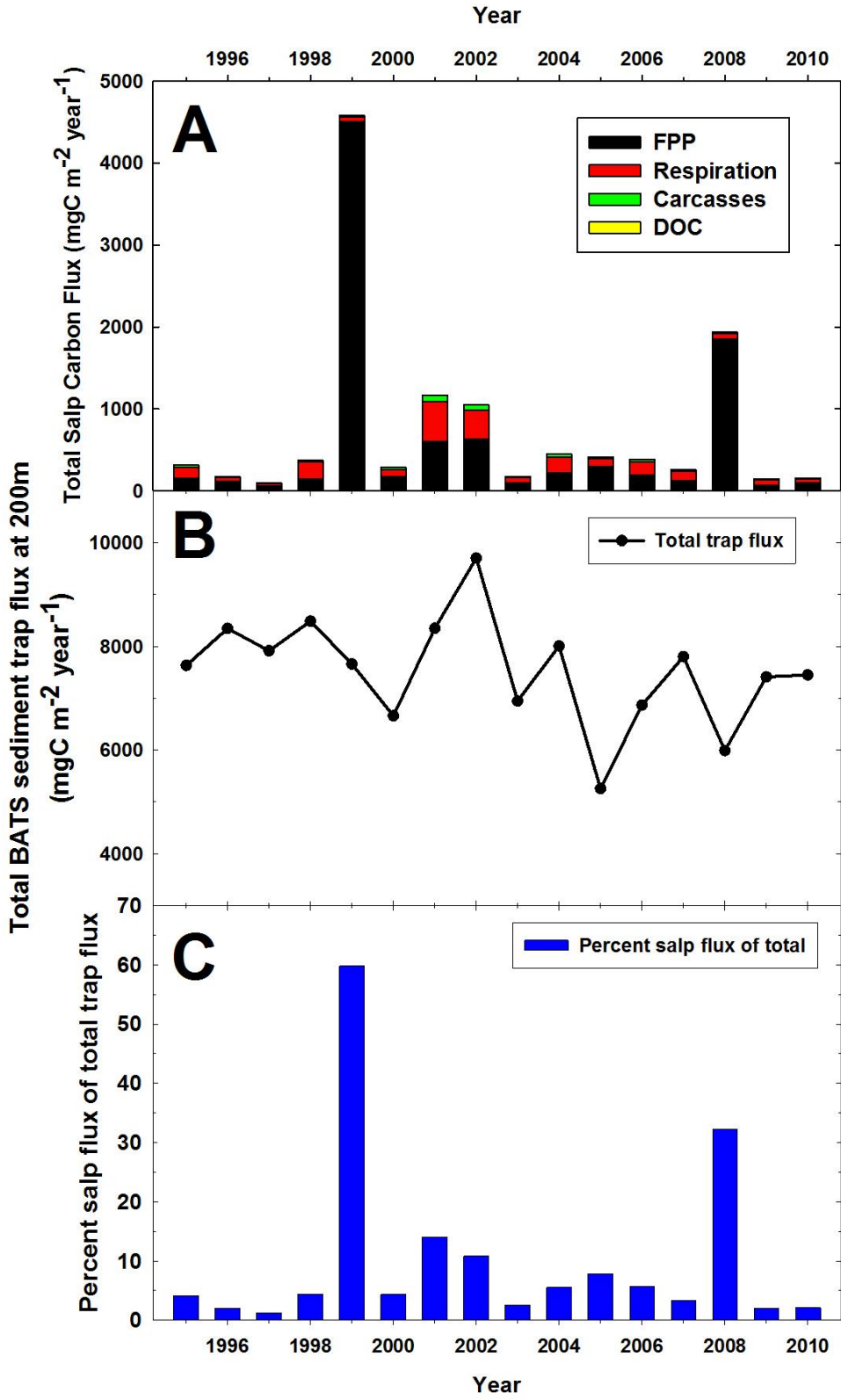


Figure 8

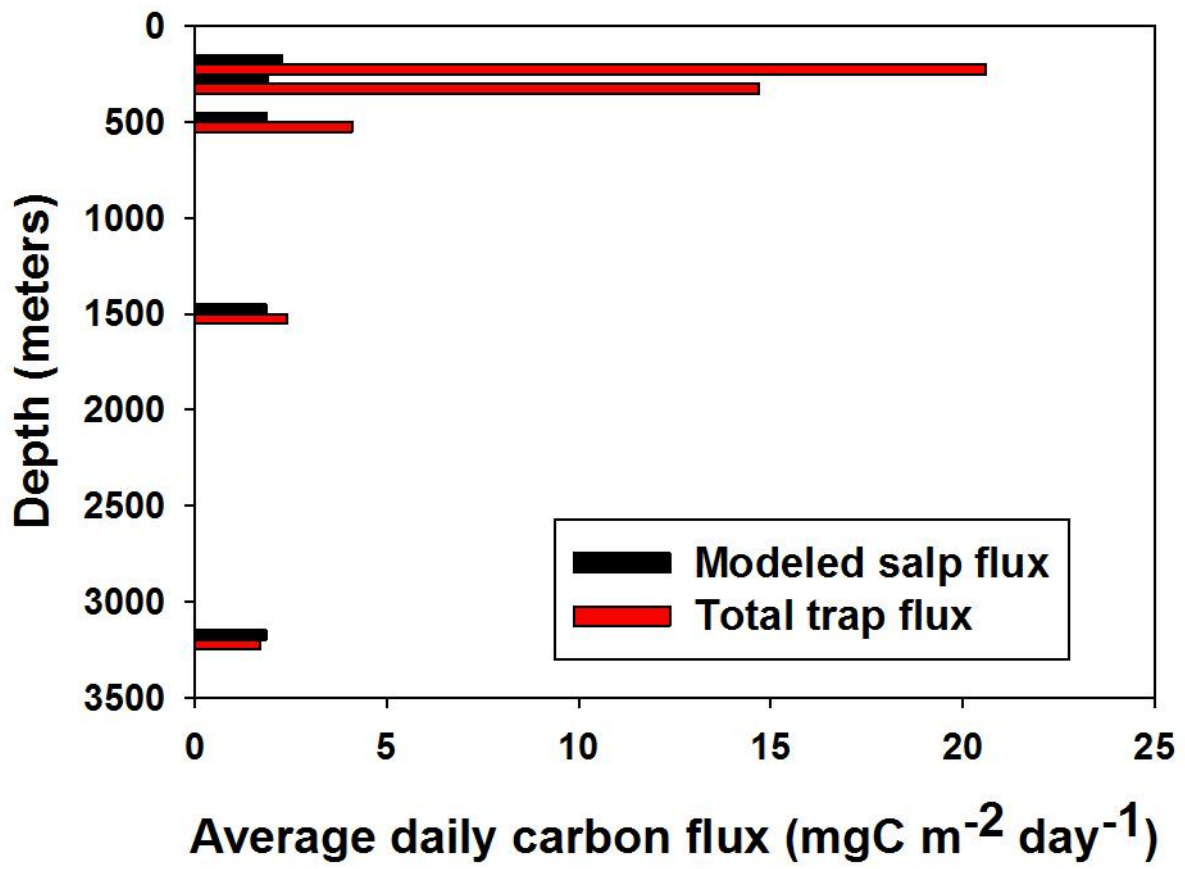


Figure 9